Graphene-MoS_2-Au-TiO_2-SiO_2 Hybrid SPR Biosensor for Formalin Detection: Numerical Analysis and Development

Md. Biplob Hossain[1,*], Mehedi Hassan[2], Lway Faisal Abdulrazak[3], Md. Masud Rana[4], Md. Mohaiminul Islam[2], M. Saifur Rahman[4]

[1]*Department of Electrical and Electronic Engineering, Jashore University of Science and Technology, Jashore, Bangladesh*
[2]*Department of Electrical and Electronic Engineering, Bangladesh Army University of Engineering and Technology, Bangladesh*
[3]*Department of Computer Science, Cihan University-Slemani, Sulaimaniya, Iraq*
[4]*Department of Electrical & Electronic Engineering, Rajshahi University of Engineering & Technology, Rajshahi, Bangladesh*

*Corresponding author: E-mail: biplobh.eee10@gmail.com; Tel: (+88) 01717 759838

Received: 06 January 2019, Revised: 20 February 2019, Accepted: 21 February 2019

DOI: 10.5185/amlett.2019.0001
www.vbripress.com/aml

Abstract

In this letter, a surface plasmon resonance (SPR) biosensor is numerically investigated that used Graphene-MoS_2-Au-TiO_2-SiO_2 hybrid structure for the detection of formalin. This developed sensor sensed the presence of formalin based on attenuated total reflection (ATR) method by observing the change of "surface plasmon resonance (SPR) angle versus the change of minimum reflectance" attributor and "the surface plasmon resonance frequency (SPRF) versus maximum transmittance" attributor. Chitosan is used as probe legend to perform particular reaction with the formalin (formaldehyde) as target legend. Here, graphene as well as MoS_2 are used as biomolecular recognition element (BRE), TiO_2-SiO_2 bilayer as the improvement of sensitivity and Gold (Au) as the sharp SPR curve. Numerical results are appeared that the variation of SPRF and SPR angle for improper sensing of formalin is quite negligible that confirms absence of formalin whereas for proper sensing is considerably countable that confirms the presence of formalin. It is also shown that the sensitivity of conventional SPR sensor is 70.74% and the graphene–MoS_2-based sensor is enhanced to 77% with respect conventional SPR sensor. The sensitivity is further enhanced to 79 % by including TiO_2–SiO_2 composite layer with respect to conventional SPR sensor. At the end of this letter, a comparative study of the sensitivity of the proposed work with the existing works is discussed.

Keywords: Biosensor, surface plasmon resonance, formalin detection, resonance angle, resonance frequency.

Introduction

Nowadays, Biosensors have been intensely researched owing to their importance of many industry applications such as medical diagnosis, enzyme detection, food safety and environmental monitoring [**1**, **2**]. Today, myriad number of biosensors have been technologically advanced, among them surface plasmon resonance (SPR) biosensor bears the advantage of compactness, light weight, high sensitivity, the case of multiplexing and remote sensing and so forth [**3**]. SPR sensor operates on the basis of attenuated total reflection (ATR) method. The ATR method uses a property of total internal reflection resulting in a momentary wave normally known as surface plasmon waves (SPW). A beam of incident light is passed through the ATR crystal in such a way that it reflects at least once off the internal surface in contact with the sample. This reflection forms the momentary wave which extends into the sample [**1**]. SPR is a momentary guided electromagnetic wave that propagates along a metal-dielectric interface. The variation of the biomolecules concentration on account of chemical reaction, will produce the local modification of the surrounding refractive index (RI) near the sensor surface that outcomes in altering the propagation constant of the SPW and thus the SPR angle and SPR frequency (SPRF) changes [**4**]. The SPR technique has been successfully applied in various fields, such as chemical and biochemical sensing, film characterization and beam characterization.

Though many materials have been used in the modeling of SPR based sensors but the two dimensional (2D) nanomaterials have taken great attention for last few years. Because of the unique optical, electronic, and catalytic properties, 2D nanomaterials have been

used in novel biosensing applications [**5**]. Graphene is one of the most extensively used 2D nanomaterial since it was discovered by K.S. Novoselov *et al.* [**6**]. It is the thinnest, strongest, transparent, self -polarization effect, ultralow phase distortion, relative high nonlinearity, tunable semiconductor, good thermal conductor, and large optical absorption [**7**]. The graphene-based SPR sensors are selected for the biosensing application, such as single-stranded DNA (ssDNA) or pseudomonas, because graphene has large surface to volume ratio which is suitable for making contact with analytes [**8**]. Another reason is that graphene surface can selectively detect aromatic compounds through pi-stacking force [**9**]. Although, a decrease in detection accuracy results, as graphene produces excessive damping in SPs due to large imaginary dielectric constant, in case of higher graphene layers [**10**].

Considering the high-performance of SPR biosensor, devices based on hybrid materials containing graphene and light-sensitive materials have brought extensive attention to researchers. This hybrid material system encompasses both the high carrier mobility of graphene and the strong absorption coefficient of the light-sensitive materials; therefore, simultaneously maximizing light harvesting and photo induced carrier extraction [**11**]. Intriguingly, another class of 2D materials that belongs to the transition-metal dichalcogenide (TMDC) [**12**] such as MoS_2, are being preferred by the biosensing fraternity [**13**], due to their large band gap [**14**], high optical absorption efficiency and large work function (5.1 eV) when combined with graphene.

The single-layered MoS_2, referred to as "beyond graphene" 2D nanocrystals material has been subjected to a good deal of attention. As a result of the quantum confinement effects, the monolayer MoS_2 has a direct bandgap of 1.8 eV, whereas bulk MoS_2 has an indirect bandgap of 1.2 eV [**15**]. Evidently, a MoS_2 enhanced hybrid nanostructure SPR biosensor can substantially improve detection limit of the device by means of the phase modulation technique.

Formalin (40% formaldehyde) is a toxic element soluble in water, has been classified as Group I Carcinogen to human beings by the International Agency for Research on Cancer (IRAC) [**16**]. Recent news and research has claimed the use of formaldehyde in food preservation that is very popular, particularly in Asian countries [**16, 17**]. As a result, the detection of formalin is a concerned issue which is a biochemical process. Its mechanism of action for fixing lies in its ability to form cross-links between soluble and structural proteins. The resulting structure retains its cellular constituents in them in vivo relationships to each other, giving it a degree of mechanical strength which enables it to withstand subsequent processing, as reported by Environmental and Occupational health and Safely Services 2004 [**16**].

Many conventional methods are available for the detection of formaldehyde such as Gas chromatography-mass spectrometry (GC-MS), high performance liquid chromatography (HPLC), fluorimetry, Nash test, gravimetric methods and other chemical based biosensors [**18-21**]. Colorimetric detection methods such as Deniges and Eegriwes methods have been known since the beginning of the 20th century [**4**]. Unluckily, these methods, reagents and reaction products are often just as harmful to human health. All of these conventional methods require similarly hazardous reagents and suffer from a number of interferences, resulting in false positions. Additionally, these methods are impracticable for real time measurements [**16**].

In this article, numerically Graphene-MOS_2-Au-TiO_2-SiO_2 pentasite layer based SPR biosensor is developed for formalin detection which results in faster immobilization by monitoring the change of SPR angle-minimum reflectance attributor and SPR frequency-maximum transmittance attributor. We used Graphene-MoS_2-Au-TiO_2-SiO_2 hybrid layer because graphene has high adsorption ability and optical characteristics, MoS_2 has high fluorescence quenching ability [**22**], and TiO_2 & SiO_2 have incredible plasmonic effect enabling effective light trapping. These effective light trapping generates more surface plasmons (SPs) which drive enhance SPR angle and frequency. This rise of SPR angle and frequency causes increase the SPR performance (sensitivity) [**23**]. This sensor is sensed the presence the formalin based on molecular concentration that is varied due to the immobilization of probe molecule (chitosan) on the sensor surface that changes the RI of sensing analytes. The RI change will in turn prime to change in the SPR angle and SPR frequency attributor that explains a change in propagation constant of SPW [**4**].

The letter is organized as follows. In section II, the design consideration and theoretical model of the proposed work is presented. In section III, the numerical results and discussion are explained under several table, equations and figures. Initial portion of the numerical results and discussion section are illustrated the detection approach and the rest discussed the sensitivity analysis.

Design consideration and theoretical model

A schematic of the proposed SPR biosensor with composite layers is shown in **Fig.1**. On the basis of kretschmann configuration of SPR, composite layer of Graphene-MoS_2-Au-TiO_2-SiO_2 have deposited on the base of prism and this whole arrangement kept in contact with the PBS or sample containing the target biomolecule/ chemical also known as analytes, for sensing application [**23**]. We used Fresnel seven layered system to design the proposed sensor which is discussed in detail in literature [**4**, **22**]. For the specification of proposed sensor, the first layer is SF11 glass prism (RI, n_p=1.7786) [**23**], second layer is TiO_2 (RI, n_2=2.5837) [**24**], third layer is SiO_2 (RI, n_3=1.4570) [**23**], fourth layer is Au (RI, n_4= 0.1838+i*3.4313) [**25**], fifth layer is MoS_2(RI, n_5=5.9+i*0.8) [**23**], sixth layer is graphene (RI, n_6=3.0

+ i 1.1487) [**23**] and final layer is Phosphate buffer saline (PBS) solution(RI n_7=1.34) as bare sensing dielectric medium that's affords better adsorption of biomolecules [**22**]. There is a number of deposition technique to deposit hybrid layer coat on the prism surface. Here, Nanostructured periodic and non-periodic plasmonic coatings including metal particles of various shapes and sizes, metal nanoshells, nanorings, periodically arranged nanostructures, have been experimentally used to deposit on photonic crystal [**26**]. Today many methods are available to prepare this nano-patterned material Graphene-MoS_2-Au-TiO_2-SiO_2) exist which have been experimentally described in literature [**26**]. Nevertheless, nanostructured periodic and non-periodic plasmonic coating still provide some advantages such as lower cost, high spatial resolution, and better surface sensitivity [**26**]. The SP field is more tightly concentrated at the vicinity of the sensor surface in the case of nanostructured periodic and non-periodic plasmonic coatings [**26**].

After finalizing the modeling, a TM polarized He-Ne (wavelength = 633 nm) light wave is used to incident as depicted in **Fig. 1**, which passes through the prism and some portion is reflected at the prism-gold interface. During intruding light energy to prism-gold interface, a momentary wave is generated which is known as surface plasmon wave (SPW) mentioning in introduction section. The SPW propagates with the dissimilar propagation constant from wave which is defined by Eq. 3. The propagation constant of SPW is varied due to the immobilization of formalin (target legend) into chitosan (probe legend which is presence in sensing analytes), and once being equal to the propagation constant of incident light. The point at which incident light propagation constant equals the SPW propagation constant is called SPR point [**4**]. SPR angle is a RI dependent parameter of sensing medium that is defined by Eq. (1). At SPR point, the frequency at which SPW propagates is called surface plasmon resonance frequency (SPRF) and the angle of incidence is called SPR angle that can be given as follows:

$$\theta_{SPR} = a\sin\sqrt{\frac{n_{com}^2 n_s^2}{n_p^2\left(n_{com}^2+n_s^2\right)}} \quad (1)$$

Here, n_{com} refers equivalent RI of Graphene-MoS_2-Au-TiO_2-SiO_2 composite layer define as $n_{com} = \sqrt{n_2 n_3 n_4 n_5 n_6}$. When formalin is flowing through chitosan on the sensor surface according to the **Fig. 1**, then the RI of sensing medium is altered due to performing chemical reaction as follows [**4**]:

$$n_s^2 = n_s^1 + C_a \frac{dn}{dc} \quad (2)$$

Here, n_s^1 is the refractive index (RI) of the sensing dielectric before adsorption of formaldehyde molecules. When dielectric sample (probe or target) is absent inside the sensing medium then n_s^1 is the RI of PBS saline (n_7=1.34) which is available in bare sensor. C_a is the concentration of adsorbed bio molecules, for example if 1000 nM concentrated formaldehyde molecules has been added into the sensing medium, then the value of C_a=1000 nM. The $\frac{dn}{dc}$ is the RI increment parameter, suppose, after adding 1000 nM concentrated formaldehyde molecules, the RI of sensing layer has been changed because the sensing layer now consists not only PBS but also formaldehyde. The changed value of RI from PBS is $\frac{dn}{dc}$ (= 0.181 cm^3/gm for PBS as bare case [**22**]). And n_s^2 is the RI of the sensing dielectric after adsorption of formaldehyde molecules. If SPR angle varies, the propagation constant of SPW also changes which was demonstrated mathematically in the literature [**3**] as given below:

$$K_{SPW} = \frac{2\Pi}{\lambda} n_p \sin\theta_{SPR} \quad (3)$$

And finally if propagation constant of SPW changes then it makes the surface resonance frequency (SPRF) to be changed which can be explained by the following equation:

$$SPRF = \frac{c_0}{n_{com}} \frac{K_{SPW}}{2\Pi} \quad (4)$$

where, $\frac{c_o}{n_{com}}$ is the propagation velocity of SPW that is a perpendicularly confined evanescent electromagnetic wave [**27-28**].

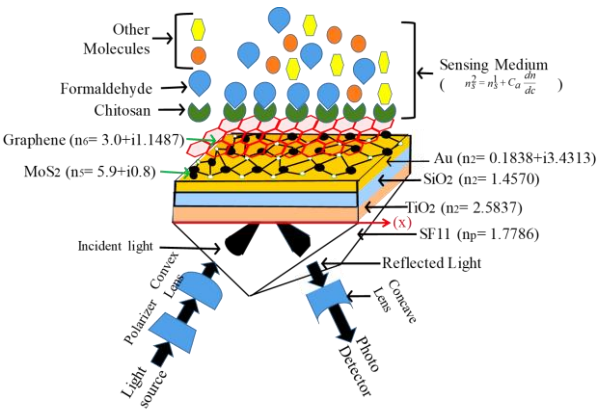

Fig. 1. Schematic of Graphene-M_OS_2-Au-TiO_2-SiO_2 Model for Mechanism of Formalin Detection with Hybrid Layer Biosensor.

If the incident angle of wave is tuned, SPR condition is achieved in which reflectance (R) of reflected wave is minimum and transmittance (T) is maximum and then then SPW penetrate at SPF along the x-direction. We define two plots, one is "transmittance versus surface resonance frequency (T~SRF curve)," as well as another is "Reflectance versus surface resonance angle (R~SPR-angle curve)," as surface resonance attributor. The sensor's performance is evaluated in terms of sensitivity(S) [**8**] which is defined as:

$$S = \frac{\Delta\theta_{SPR}}{\Delta n^2{}_s} \quad (5)$$

Here, $\Delta\theta_{SPR}$ is the change of SPR angle due to the presence of formalin and Δn_s^2 is the change of RI of the sensing dielectric after adsorption of formalin.

Numerical results and discussion

Numerical analysis has been commenced to check the routine of proposed sensor by finding it surface plasmon resonance (SPR) angle versus the change of minimum reflectance (R~SPR-angle)" attributor and "the surface plasmon resonance frequency (SPRF) versus maximum transmittance (T~SPRF)" attributor curve. **Fig. 2(a)** and **2(b)** are demonstrating R~SPR-angle and T~SPRF curve. The angle of incidence and SPRF of bare sensor are 56.26^0 and 97.968THz respectively. And the angle of incidence and SPRF while 1000 nM probe chitosan are placed on sensing dielectric, are 56.34^0 and 98.688 THz respectively. Results show no noteworthy change in SPR angle and SPRF (change of SPR angle is 0.080, change of SRF is 0.72 THz only) since there no bonding has taken place between probe and target due to the absence of formalin.

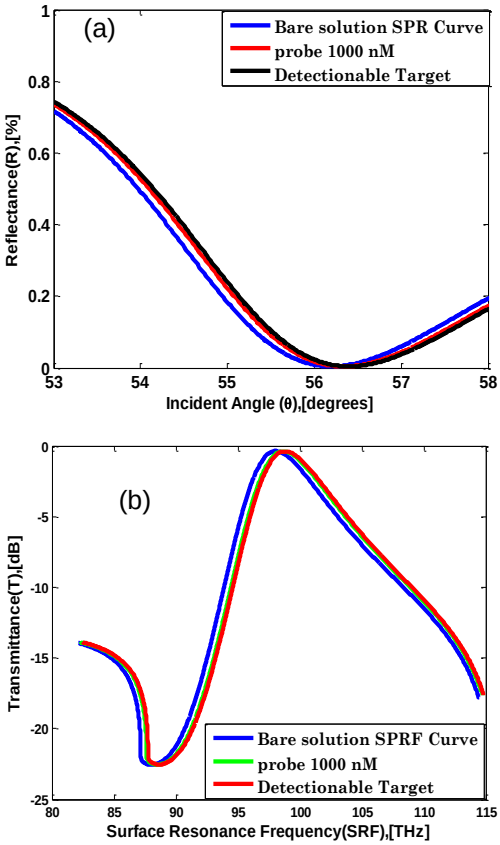

Fig. 2. Numerical results of Bare SPR Sensor (a) R~SPR-angle curve in the absence of formalin and chitosan. (b) T~SPRF curve in the absence of formalin and chitosan.

Fig. 3 reveals the final stage of detection concept. It shows, the change of attributor (θsp & R_{min}) and (ΔSPRF &T_{max}) while 1000 nM formaldehyde molecule is sinking in the probe. Results suggest significant change in SPR angle as well as SPRF (58.05^0 and 99.875 THz) due to bonding has taken place between probe (chitosan) and target (formalin) legend shown in **Fig. 1**. So there is considerable change of charges in target molecule.

Table 1. R_{min} [%], θ_{SP}[deg] , T_{max}[dB] and SPRF[THz] for different concentrated dielectrics medium.

Concentration (C_a) [nM]	R_{min} [%]	θ_{SP} [deg]	T_{max} [dB]	SPRF [THz]
1000 (immobilizer Probe)	0.0044	56.3400	0.3795	98.688
1000 (Detectionable Target)	0.0062	58.0500	0.3981	99.875
1001 (Detectionable Target)	0.0066	58.3800	0.4002	100.008
1010 (Detectionable Target)	0.0070	58.6700	0.4018	100.106
1100 (Detectionable Target)	0.0082	59.4900	0.4106	100.627
1110 (Detectionable Target)	0.0085	59.6800	0.4129	100.761
1200 (Detectionable Target)	0.0100	60.6200	0.4249	101.447

The change of detecting attributor (θsp&R_{min}) and (ΔSPRF &T_{max}) owing to adding formalin is provided in **Table 1**. The amount of shift moves forward with increasing concentration of the detectionable target from 1 to 200 nM as stated by Eq. 2 and tabulated in **Table 1**. The information of **Table 1** has been extracted from **Fig. 3(a)** and **3(b)**.

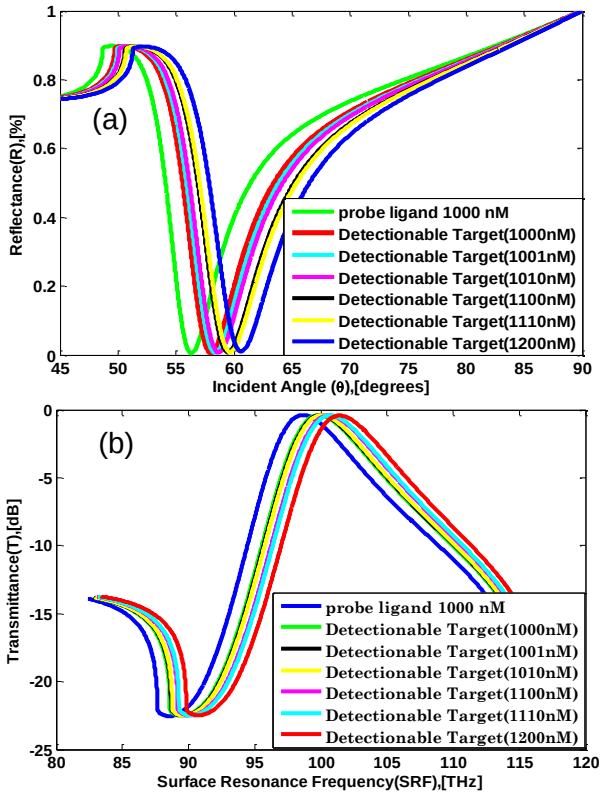

Fig. 3. (a) Reflectance vs. Incident Angle Curve and (b) Transmittance vs. SPR Frequency Curve for Different Concentration of Detectionable Target.

Table 1 gives information about how θSPR and SPRF parameters vary with different concentrations of formalin molecules.

It is apparently seen that the considerable increase of SPR angle and SPRF is a sign of bonding between probe and target.Upon making a bond with the target, the chemical configuration of legend is changed, which leads to the change in the optical properties. Thus, we can observe whether there is formalin in the sample or not. Also increased amount of formalin forms more recurring bonds thus indicating greater interaction [**29, 30**]. To draw a decision, at first we measure and

tabulate the values of ΔR_{min}^{P-T} and $\Delta\theta_{sp}^{P-T}$ in **Table 2** and compare these to threshold values ((ΔR_{min}^{P-T})$_{\min}$ and ($\Delta\theta_{sp}^{P-T}$)$_{\min}$). If the measured values are greater than these threshold values, then we can say there ispresence of formalin in the sample. The following equations describe the threshold parameters:

$$\Delta(R_{\min}^{P-T})_{\min} = \left|R_{\min}^{Probe} - R_{\min}^{Target}\right| = 0.0018 \quad (6)$$

$$\Delta(\theta_{SP}^{P-T})_{\min} = \left|\theta_{SP}^{Probe} - \theta_{SP}^{Target}\right| = 1.71[Deg] \quad (7)$$

where, (ΔR_{min}^{P-T})$_{\min}$ is the threshold value of minimum changed reflectance, ($\Delta\theta_{sp}^{P-T}$)$_{\min}$ is the threshold value of changed SPR angle, R_{min}^{Probe}represents the minimum reflectance of probe legend (chitosan), R_{min}^{Target}denotes the minimum reflectance of sampling target, θ_{sp}^{Probe} depicts the SPR angle of probe legend and finally SPR θ_{sp}^{Target} is the SPR angle of sampling target. We reached and tabulated the same calculation by taking $\Delta SPRF_{p-T}$ and ΔT_{max}^{p-t} as also the detecting attributors. The following equations are used to determine the threshold values of these attributors as:

$$\Delta(T_{\max}^{P-T})_{\min} = \left|T_{\max}^{Probe} - T_{\max}^{Target}\right| = 0.0186 \quad (8)$$

$$\Delta(SRF_{P-T})_{\min} = \left|SRF_{probe} - SRF_{target}\right| = 1.187 \quad (9)$$

The numerical data justifies the strong dependency of the SPR angle and SPRF on the concentration increment that reflects in reflectance and transmittance characteristics curve. These acquired numerical values can really give an option about successful interaction or the failed ones.

Table 2. Calculated ΔR_{min}^{P-T} [%], ΔT_{max}^{p-t} , ΔSRF_{p-t} [THz] and $\Delta\theta_{sp}^{P-T}$ [deg] values from Eq. 5 to Eq. 8 for different concentration of dielectric medium.

Concentration (C_a) [nM]	ΔR_{min}^{P-T}[%] = $\lvert R_{min}^{Probe} - R_{min}^{Target}\rvert$	$\Delta\theta_{sp}^{P-T}$[deg] = $\lvert\theta_{sp}^{Probe} - \theta_{sp}^{Target}\rvert$	ΔT_{max}^{p-t} [dB] = $\lvert T_{max}^{p} - T_{max}^{t}\rvert$	ΔSRF_{p-t} [TH = $\lvert SRF_p - SRF_t\rvert$
1000 (Target)	(ΔR_{min}^{P-T})$_{\min}$	($\Delta\theta_{sp}^{P-T}$)$_{\min}$	($\Delta T_{\max}^{p-t}$)$_{\min}$	(ΔSRF_{p-t})$_{\min}$
1001 (Target)	0.0022	2.04	0.0207	1.32
1010 (Target)	0.0026	2.33	0.0223	1.418
1100 (Target)	0.0038	3.15	0.0311	1.939
1110 (Target)	0.0041	3.34	0.0334	2.073
1200 (Target)	0.0056	4.28	0.0354	2.759

The first condition in **Table 3** expresses the desired condition, second and third one require careful recheck for attaining desired condition, fourth condition confirms the probe is still free from formalin molecule. As a second factor, we determine the improvement of sensitivity of the proposed SPR optical biosensor. The SPR angle soars with the increment of refractive index according to Eq.1. The variation of sensitivity of the proposed biosensor with respect to the increment of refractive index with a RI step Δn = 0.01 RIU is measured and tabulated in **Table 4** and its corresponding results is graphically shown in **Fig. 4**.

Table 3. Four Probable Conditions for Making Decision about Successful Interaction.

Conditions for using & R_{min} as detecting attributor	Conditions for using ΔSPRF &T_{max} as detecting attributor	Decision
$\Delta R_{min}^{P-T} \geq (\Delta R_{min}^{P-T})_{\min}$ && $\Delta\theta_{sp}^{P-T} \geq (\Delta\theta_{sp}^{P-T})_{\min}$	$\Delta T_{max}^{p-t} \geq (\Delta T_{max}^{p-t})_{\min}$ && $\Delta SRF_{p-t} \geq (\Delta SRF_{p-t})_{\min}$	Formalin is detected
$\Delta R_{min}^{P-T} \geq (\Delta R_{min}^{P-T})_{\min}$ && $\Delta\theta_{sp}^{P-T} \leq (\Delta\theta_{sp}^{P-T})_{\min}$	$\Delta T_{max}^{p-t} \geq (\Delta T_{max}^{p-t})_{\min}$ && $\Delta SRF_{p-t} \leq (\Delta SRF_{p-t})_{\min}$	Re-evaluate
$\Delta R_{min}^{P-T} \leq (\Delta R_{min}^{P-T})_{\min}$ && $\Delta\theta_{sp}^{P-T} \geq (\Delta\theta_{sp}^{P-T})_{\min}$	$\Delta T_{max}^{p-t} \leq (\Delta T_{max}^{p-t})_{\min}$ && $\Delta SRF_{p-t} \geq (\Delta SRF_{p-t})_{\min}$	Re-evaluate
$\Delta R_{min}^{P-T} \leq (\Delta R_{min}^{P-T})_{\min}$ && $\Delta\theta_{sp}^{P-T} \leq (\Delta\theta_{sp}^{P-T})_{\min}$	$\Delta T_{max}^{p-t} \leq (\Delta T_{max}^{p-t})_{\min}$ && $\Delta SRF_{p-t} \leq (\Delta SRF_{p-t})_{\min}$	Free Probe

Table 4. Arrangement of sensitivity corresponding to sensing layer refractive index from 1.34 to 1.41 for seven different structures at the optimum thickness of TiO_2, SiO_2 and monolayer of MoS_2 and graphene.

Structure configuration	Sensitivity (s) [%RIU^{-1}]							
	n_s^2 =1.34	n_s^2 =1.35	n_s^2 =1.36	n_s^2 =1.37	n_s^2 =1.38	n_s^2 =1.39	n_s^2 =1.40	n_s^2 =1.41
Conventional	70.44	70.54	71.12	72.00	72.96	73.38	74.14	75.26
Conventional with Graphene	71.62	71. 76	72.18	73.08	73.88	74.22	75.74	76.24
Conventional with MoS_2	76.44	75.84	76.36	77.28	78.14	79.32	80.00	81.82
Conventional with Graphene-MoS_2	77.00	77.26	77.76	78.22	79.32	80.12	81.54	82.40
Conventional with Graphene-MoS_2-TiO_2	78.00	78.00	79.08	80.10	81.00	82.80	83.70	85.14
Conventional with Graphene-MoS_2-SiO_2	77.00	75.90	77.66	78.02	79.12	79.98	81.34	82.10
Conventional with Graphene-MoS_2-TiO_2-SiO_2 (Proposed)	79.00	78.80	79.70	80.40	81.90	83.00	84.00	85.40

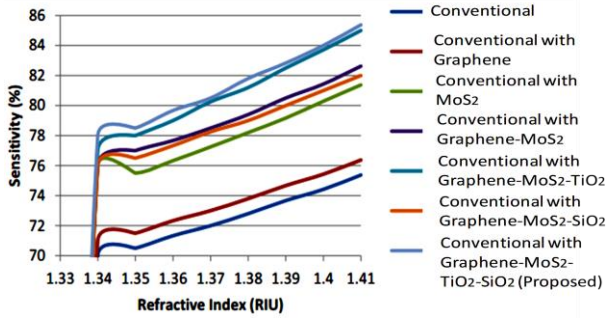

Fig. 4. Sensitivity [%] vs. Refractive Index [RIU] graph for different Layer Structure.

We compare the main performance parameter i.e. sensitivity with different sensor structure for 1.34 RIU refractive index (PBS). From **Fig. 4**, it can easily be observed that the sensitivity without TiO_2, SiO_2, MoS_2 and Graphene (conventional structure) is very poor and 70.44% whereas the sensitivity with graphene but without TiO2, SiO_2 and MoS_2 layers is 71.62% consistently better than the conventional structure. This

is due to the electron loss of graphene, which is accompanying with the imaginary dielectric constant. This increased SPR angle will lead to obtain increased sensitivity of the sensor as sensitivity is directly related to the variation of SPR angle discussed in ref. [**31**]. Furthermore, the sensitivity without TiO_2, SiO_2 and graphene but with MoS_2 layer is 76.44%. Because of MoS_2's larger band gap [**32**], higher optical absorption efficiency [**33, 34**] and larger work function (5.1 eV) as equated with graphene [**35**].

The sensitivity of the quantum-confinement-incurred direct band gap in MoS_2, allows the high sensitive detection of bio targets. It also holds high fluorescence quenching ability and different affinity in the direction of bio targets [**36**, **37**]. After more if both graphene and MoS_2 are used and TiO_2 and SiO_2 layers are not used then sensitivity improves to 77%. This greater than before performance is due to the absorption ability and optical characteristics of graphene biomolecules and high fluorescence quenching ability of MoS_2. Further again, if TiO_2-SiO_2 composite layer is used with the Graphene & MoS_2 then the sensitivity enhances from 77% to 78%. Titanium dioxide (TiO_2) and SiO_2 have purely real refractive index; hence, can be used as adherence layer above the prism base. As an adherence layer, the composite layer performs better than the individual TiO_2 and SiO_2 [**38**, **39**] because rich plasmon happens at the TiO_2–SiO_2 interface [**40**]. And this plasmon enhances light trapping effectively [**41**] which will generate more surface plasmons (SPs). Due to this more surface plasmons (SPs), which will enhance the SPR angle. This increase in SPR angle will increase the SPR sensitivity. Finally, the sensitivity for the proposed structure has been carried out, and result is 79%, the highest value among all the previous structures. In order to assimilate the advantages of graphene, MoS_2, TiO_2 and SiO_2, we are motivated to use all of them in a single biosensor, which increases the sensitivity.

Third important factor is to investigate the electric field distribution along the normal to the interface. We applied finite difference time domain (FDTD) method to know electric field distribution, by using commercial software Lumerical FDTD solution. The FDTD is a powerful method to solve Maxwell's equations in a nano film layer by using YEE-algorithms. The FDTD method is a more reliable than others, such as multiple-multiple or Green's dynamic method in solving Maxwell's equations for complex geometries and dispersive media, such as gold and silver [**42**]. The simulation was carried out with the Gaussian-modulated continuous wave with the center wavelength of 633 nm. Surface plasmon polarition (SPP) excitation is performed using wavelength interrogation technique. To simulate the sensor configuration, we consider the thickness of prism is (d_1) =50 nm, the thickness of TiO_2 is (d_2) =37 nm, the thickness of SiO_2 is (d_3) =20 nm, the thickness of gold is (d_4) = 46 nm, the thickness of monolayer MoS_2 is (d_5) =0.65 nm and the thickness of monolayer graphene is (d_6) = 0.34 nm [**23**]. Field intensity was reported using DFT reflectance and transmission monitor at 250 nm away from graphene/sensing medium interface.

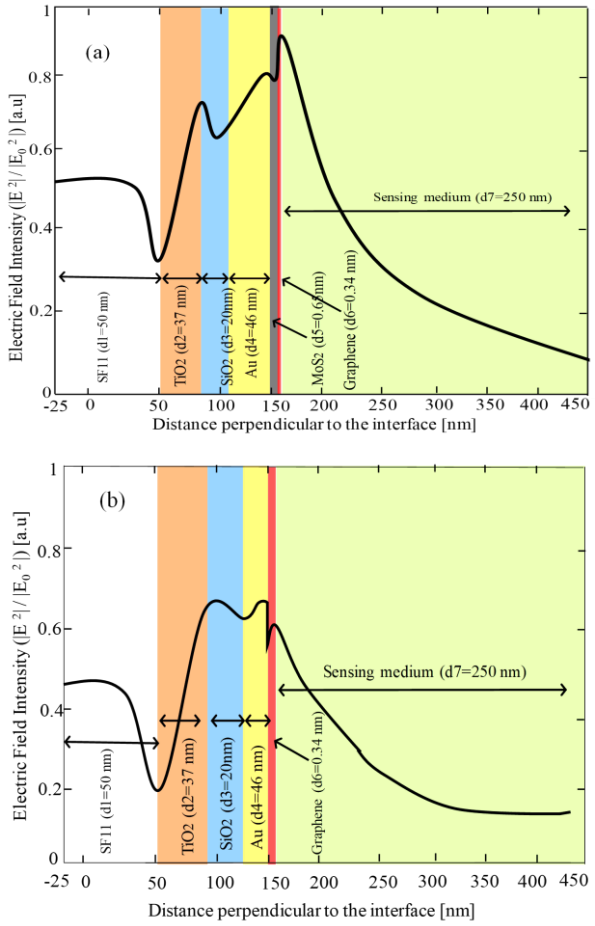

Fig. 5. The electric field intensity in the direction of x axis along the perpendicular to the interface for the structure (a) with MoS_2 layer and (b) without MoS_2 layer.

The intensity of the field approaches maximum at the instant of minimum reflectivity due to maximum excitation of SP takes place [**23**]. In **Fig. 5**, we observe that the highest field is originated at the MoS_2–graphene interface due to most plasmonic effect arises near this interface which in turn rises the sensitivity of the proposed structure. Moreover, Au layer improves the field gradually till to gold–MoS_2 interface which represents the excitation of SPs at this interface. The field intensity drops suddenly in the SiO_2 and then nonstop to decrease at gradual rate.

Electric field intensity in two configurations of the proposed biosensor structure with MoS_2 layer in **Fig. 5(a)** and no MoS_2 layer in **Fig. 5(b)** have been compared. It is easily being seen from **Fig. 5(a)**, the numerical values of the electric field intensity in the configuration with MoS_2 layer is greater than the configuration without MoS_2 layer. The electric field distribution is plotted for incident angle of 60.62° (SPR angle) while 1200 nM concentrated formalin is present.

Lastly, we feel like making a Table showing a comparison of sensitivity of the proposed SPR sensor with other existing. **Table 5** has been made with taking into account of sensitivity, on the basis of Structure configuration, and operating wavelength sensors in the literature.

Table 5. Sensitivity of the proposed work and comparison with other existing works.

Structure configuration	**Sensitivity [Deg-RIU^{-1}]**	**Wavelength (nm)**	**Reference**
Conventional with Graphene-MoS_2-TiO_2-SiO_2	79.00	633	In this study
Graphene Coating	57.14	633	[43]
Au-Aluminum thin coating	9.56	680	[44]
graphene sheet coated on silver with chromium substrate	68.03	633	[10]
Gold-silver bimetallic film	54.84	632.8	[3]
Au-Graphene-MoS_2 hybrid	89.29	1024	[30]

Conclusion

In this work, a numerical analysis is reported to observe the effect of adding of graphene, MoS_2, TiO_2 and SiO_2 layer step by step on sensitivity parameters for formalin detection. The first feature of this study is to detect the presence the formalin based on attenuated total reflection (ATR) method by observing the change of "surface plasmon resonance (SPR) angle versus the change of minimum reflectance" attributor and "the surface plasmon resonance frequency (SPRF) versus maximum transmittance" attributor. Here, Chitosan is used as probe legend to perform particular reaction with the formalin (formaldehyde) as target legend. The second principle feature of this SPR biosensor is the use of graphene, MoS_2, TiO_2 and SiO_2 to enhance the sensitivity. The proposed biosensor has a greater sensitivity of 79.00 Deg-RIU^{-1} as compared to the other reported conventional SPR biosensor. Hence, for the first time as per the best of our knowledge, numerical analysis of Graphene-MoS_2-Au-TiO_2-SiO_2 pentasite layer in a single SPR biosensor is proposed.

References

1. Pumera, M.; *Materials Today*, **2011**, *14*, 308.
2. Homola, J.; *Analytical and Bioanalytical Chemistry*, **2003**, *377*, 528.
3. Xia, L.; Yin, S.; Gao. H.; Deng, Q.; Du. C.; *Plasmonics*, **2011**, *6*, 245.
4. Hossain, M. B.; Rana, M. M.; *J. Sensor*, **2016**.
5. Zhu, C.; Zeng, Z.; Li, H.; Li, F.; Fan, C.; Zhang, H.;*J. Am. Chem. Soc.*, **2013**, *135*, 5998.
6. Novoselov, K.S.; Geim, A.K.; Morozov, S.V.; Jiang, D.; Zhang, Y.; Dubonos, S.V.; Grigorieva, I.V.; Firsov, A. A.; *Science*, **2004**, *306*, 666.
7. Hoggard, A.; Wang, L.Y.; Ma, L.; Fang, Y.; You, G.; Olson, J.; Liu, Z.; Chang, W.S.; Ajayan, P. M.; Link, S.; *ACS Nano*, **2013**, *7*, 11209.
8. Verma, A.; Prakash, A.; Tripathi, R.; *Opt. Quant. Elect.*, **2014**, *47*, 1197.
9. McGaughey, G.B.; Gagne, M.; Rappe, A. K.; *J. Biol. Chem.* **1998**, *273*, 15458.
10. Alka, V.; Prakash, A.; Rajeev, T.; *Optics Communications*, **2015**, *357*, 106.
11. Banxian, R.; Jun, G.; Leiming, W.; Jiaqi, Z.; Qi, Y.; Xiaoyu, D.; Yuanjiang, X.; *Sensors*, **2017**, *17*, 1924.
12. Maharana, P. K.; Jha, R.; *Sens. Actuators B*, **2012**, *169*,161.
13. Kin, F. M.; Changgu, L.; James, H.; Jie, S.; Tony, F. H.; *Phys. Rev. Lett.*, **2010**, *105*, 136805.
14. Ouyang, Q.; Zeng, S.; Dinh, X. Q.; Coquet, P.; Yong, K.T.;*Procedia Engineering*, **2016**, *140*, 134.
15. Mishra, A. K.; Mishraand, S. K.; Verma, R.K.; *J. Phys. Chem. C*, **2016**, *120*, 2893
16. Aini, B. N.; Siddiquee, S.; Ampon, K.; *Biosensors*, **2016**, *63*.
17. Marzuki, N.I.; Bakar, F.A.; Salleh, A.B.; Heng, L.Y.; Yusof, N.A.; Siddiquee, S.; *Int. J. Electrochem. Sci*. **2012**, *7*, 6070.
18. Noordiana, N.; Fatimah, A.B.; Farhana, Y.C.; *Int. Food Res. J.*, **2011**, *18*, 125.
19. Bechmann, I.E.; *Anal. Chim. Acta*, **1996**, *320*, 155.
20. Ngamchana, S.; Surareungchai, W.; *Anal. Chim. Acta*,**2004**, *510*, 195.
21. Yeh, T.S.; Lin, T.C.; Chen, C.C.; Wen, H.M.; *J. Food Drug Anal*., **2013**, *21*, 190.
22. Rahman, M. S.;Anower, M. S.; Rahman, M. K.; Hasan, M. R.; Hossain, M. B.; Haque, M. I.; *Optik*, **2017**, *140*, 989.
23. Maurya, J. B.; Prajapati, Y.K.; Singh, V.; Saini, J. P.; *Appl Phys A*,**2015**, *121*, 525.
24. Jorgenson, R.C.; Yee, S.S.; *Sensors and Actuators B*, **1993**,*12*, 213.
25. Maurya, J.B.; Prajapati, Y.K.; Rajeev T.; *Silicon*, **2018**,*10*, 245.
26. Elizaveta, K.; Peipei, J.; Heike, E.-H.; Tanya, M. M.; Alexandre, F.; *Sensors*,**2016**, *17*.
27. Jorgenson, R. C.; Yee, S.S.; *Sensors and Actuators B*, **1993**, *12*, 213.
28. Nylander, C.; Liedberg, B.; Lind, T.; *Sensors and Actuators B*, **1982**, *3*, 79.
29. Fano, U.; *Journal of the Optical Society of America*, **1941**, 31, 213.
30. Earp, R.L.; Dessy, R.E.; Surface Plasmon Resonance; Commercial Biosensors: Applications to Clinical, Bioprocess, and Environmental Samples; Commercial Biosensors: Applications to Clinical, Bioprocess, and Environmental Samples; Graham, R.; James, D.W.; John Wiley and Sons: **1998**.
31. Rahman, M. S.; Anower, M. S.; Hasan, M. R.; Hossain, M. B.; Haque, M. I.; *Optics Communications*, **2017**, *396*, 36.
32. Mayorga-Martinez, C.C.; Ambrosi, A.; Eng, A.Y.S.; Sofer, Z.; Pumera, M.; *Adv. Funct. Mater*, **2015**, *25*.
33. Ambrosi, A.; Eng, A.Y.S.; Sofer, Z.; Pumera, M.;*Chem. Commun.*2015, *51*.
34. Brien, M. O', K.; Morrish, L. R.; Berner, N. C.; McEvoy, N.; Wolden, C.A.; Duesberg, G. S.; *Chem. Phys. Lett.*, **2014**, *615*.
35. Yunhan, L.; Chaoying, C.; Kai, X.; Shuihua, P.; Heyuan, G.; Jieyuan, T.; Huiui, L.; Jianhui, Y.; Jun, Z.; Yi, X.; Zhe, C.; *Opt. Express*, **2016**,*24*.
36. Shi, H.; Pan, H.; Zhang, Y.W.; Yakobson, B.I.; *Phys. Rev. B*, **2013**, *87*.
37. Maurya, J.B.; Prajapati, Y.K.; Singh, V.; Saini, J.P.; Tripathi, R.; *Opt. Quant. Electron*, **2015**, *47*, 3599.
38. Maier, S. A.; Plasmonics: Fundamentals and Applications, Springer, **2007**.
39. Schedin, F.; Lidorikis, E.; Lombardo, A.; Vasyl, G.K.; Andre, K.G.; Alexander, N.G.; Novoselov, K.S.; Ferrari, A.C.; *ACS Nano*, **2010**, *4*, 5617.
40. Reather, H.; Surface Plasmons on smooth and rough surfaces and on gratings, SpringerBerlin, **1988**, *111*.
41. Choi, S.H.; Kim. Y.L.; Byun, K. M.; *Opt. Express*, **2011**, *19*, 458.
42. Hossain, M. B.; Muktadhir, S.; Rana, M. M.; *Optik - International Journal for Light and Electron Optics*, **2016**, *127*, 5841.
43. Hossain, M. B.; Rana, M. M.; *Sensor Letters*, **2016**, *14*, 145.
44. Biednov, M.; Lebyedyeva, T.; Shpylovyy, P.; Gold and Aluminum based surface Plasmon resonance biosensors: sensitivity enhancement, Opt. Sensors Proc. 9506, **2015**.

